


CircPRMT5, a Potential Salivary Biomarker, Facilitates the Progression of Head and Neck Squamous Cell Carcinoma via the IGF2BP3-SERPINE1 Pathway

Siqi Jiang^{1,2}, Linlin Ou^{1,2}, Yueqi Wang^{1,2}, Kai Su^{1,2}, Zhipei Chen^{1,2}, Lihong He^{1,2}, Xun Xu^{1,2}, Bin Cheng^{1,2}, Juan Xia^{1,2}, Zhaona Fan^{1,2} 

¹Hospital of Stomatology, Sun Yat-sen University, Guangzhou, People's Republic of China; ²Guangdong Provincial Key Laboratory of Stomatology, Guanghua School of Stomatology, Sun Yat-sen University, Guangzhou, People's Republic of China

Correspondence: Zhaona Fan; Juan Xia, Hospital of Stomatology, Sun Yat-sen University, No. 56 Lingyuanxi Road, Guangzhou, Guangdong, 510055, People's Republic of China, Tel +86 20 87394123; +86 20 83741891, Fax +86 20 83822807, Email fanzhn3@mail.sysu.edu.cn; xiajuan@mail.sysu.edu.cn

Purpose: Circular RNAs (circRNAs) are associated with the progression of tumors and hold promise as potential biomarkers for liquid biopsy. Among these, the role of circPRMT5 in head and neck squamous cell carcinoma (HNSCC) remains to be elucidated. This study aims to examine the role and underlying mechanisms of circPRMT5 in the progression of HNSCC and to assess its potential diagnostic value in saliva exosomes.

Methods: The expression of circPRMT5 and its clinical significance in HNSCC were investigated. Both in vitro and in vivo studies were performed to elucidate the biological role of circPRMT5 in HNSCC. RNA sequencing was utilized to identify downstream mechanisms. To evaluate and validate these mechanisms, Western blotting, RNA-FISH, immunofluorescence, immunohistochemistry, RIP, and rescue experiments were employed. Finally, salivary exosomes were isolated, and the expression levels of circPRMT5 were assessed using qRT-PCR.

Results: The upregulation of circPRMT5 in HNSCC tissues was identified to be correlated with cervical lymph node metastasis and advanced clinical T stage. Both in vitro and in vivo experiments manifested that circPRMT5 promoted the proliferation and metastasis of HNSCC. Mechanistically, circPRMT5 was demonstrated to directly bind to and stabilize the insulin-like growth factor 2 mRNA-binding protein 3 (IGF2BP3), which, subsequently, binds to and stabilizes the serpin family E member 1 (SERPINE1) mRNA, thereby enhancing SERPINE1 expression. Furthermore, rescue experiments indicated that the proliferative, invasive, and migratory effects of circPRMT5 in HNSCC were dependent on the involvement of IGF2BP3 and SERPINE1. Notably, circPRMT5 levels were significantly elevated in the saliva exosomes of HNSCC patients, exhibiting substantial diagnostic value.

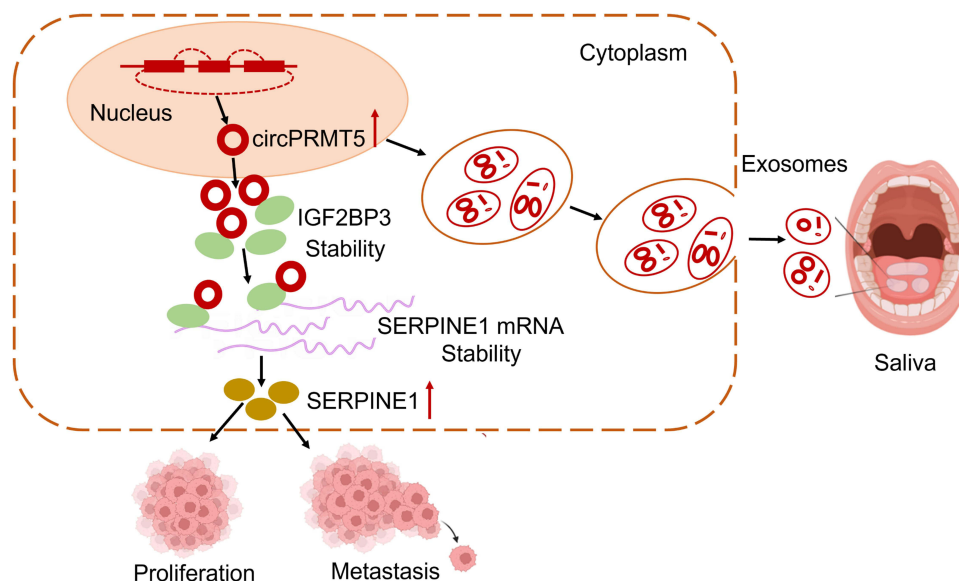
Conclusion: CircPRMT5 exhibits significant diagnostic utility through salivary exosomes and plays a crucial role in promoting the progression of HNSCC via the IGF2BP3-SERPINE1 pathway. These findings highlight the potential of circPRMT5 as a noninvasive diagnostic biomarker and a therapeutic target for patients with HNSCC.

Keywords: head and neck cancer, circPRMT5, IGF2BP3, SERPINE1, salivary exosomes

Introduction

Head and neck squamous cell carcinomas (HNSCCs), originating from the mucosal epithelium of the oral cavity, pharynx, and larynx, are the most common malignancies in the head and neck region.^{1,2} Over recent decades, multimodal treatment strategies encompassing surgery, radiotherapy, and molecular-targeted therapy have yielded significant clinical benefits for HNSCC patients.^{2,3} Regrettably, a significant proportion of patients with HNSCC present with cervical lymph node metastases, resulting in limited or suboptimal therapeutic options. As a consequence, two-thirds of HNSCC patients are diagnosed at an advanced stage, contributing to the stagnation of long-term survival rates at approximately

Graphical Abstract



50%.¹ Therefore, identifying noninvasive markers for early diagnosis and metastasis prediction, along with elucidating the molecular mechanisms of HNSCC, is crucial for improving patient prognosis.

Circular RNAs (circRNAs) are single-stranded, covalently closed RNA molecules found across a wide range of species, from viruses to mammals.⁴ Numerous indicate that circRNAs have distinct expression profiles and are involved in various diseases, highlighting their potential as diagnostic biomarkers and therapeutic targets.⁴ CircRNAs serve as transcriptional regulators, miRNA sponges, and templates for protein synthesis.^{5–7} CircRNA-protein interactions involve various mechanisms such as modulating protein-protein interactions, binding or sequestering proteins, forming circRNA-protein-mRNA ternary complexes, and translocating or redistributing proteins.^{4,5} For instance, circMTCL1 enhances C1QBP translation in laryngeal squamous cell carcinoma by directly recruiting the C1QBP protein and inhibiting its degradation through the ubiquitin-proteasome pathway.⁸ CircNEIL3 suppresses metastasis by directly interacting with YBX1, leading to its Nedd4L-mediated proteasomal degradation.⁹

Exosomes are membrane-bound vesicles with diameters typically between 40 to 160 nm, averaging around 100 nm.¹⁰ These vesicles, containing microRNA (miRNA), messenger RNA (mRNA), and proteins, are secreted by cells into the extracellular milieu.¹¹ Recent studies have shown that cancer cell-derived exosomes can release circRNAs into the bloodstream, urine, and saliva.^{12,13} Given the high abundance of salivary exosomes in patients with HNSCC, it is of considerable interest to explore the functional roles and clinical implications of circRNAs derived from HNSCC.

While circPRMT5's involvement in malignancies like bladder and lung cancer is documented, its role and mechanisms in HNSCC remain unexplored.^{14,15} This study aimed to investigate the role and underlying mechanisms of circPRMT5 in the progression of HNSCC, as well as to evaluate its diagnostic potential in salivary exosomes. The expression of circPRMT5 was found to be significantly elevated in both HNSCC tissues and the salivary exosomes of affected patients, facilitating HNSCC progression via the IGF2BP3-SERPINE1 signaling pathway. We believe these findings will contribute to the development of new potential predictive markers for HNSCC and provide a theoretical basis for the targeted therapy of HNSCC.

Materials and Methods

Ethics Statement

This study's human saliva and tissue samples were obtained from the Affiliated Stomatology Hospital of Sun Yat-Sen University in Guangzhou, China. The study received approval from the Ethics Committee (KQEC-2024-102-01). Human

samples were collected from the Inpatient Department of Oral and Maxillofacial Surgery at the Affiliated Stomatology Hospital of Sun Yat-Sen University between 2023 and 2024. After collection, the tissue samples were cryopreserved in liquid nitrogen or fixed in 4% paraformaldehyde for histological verification. Every patient signed an informed consent prior to participating in the study. This study complies with the Declaration of Helsinki.

The Institutional Animal Care and Use Committee (IACUC) at Sun Yat-Sen University has reviewed and approved the animal use protocol (SUSY-IACUC-2023-001630). This evaluation adhered to the standards of the Animal Welfare Act and the US Public Health Service's "Guide for the Care and Use of Laboratory Animals".

Cell Lines and Culture

The SCC15 human oral squamous cell line was sourced from the American Type Culture Collection (ATCC, USA), and the HN6 cell line was supplied by Southern Medical University (Guangdong, China). HN6 and SCC15 cells were cultured in DMEM/F12 medium (Gibco, USA) with 10% fetal bovine serum (Front Biomedical/BOVOGEN, Australia) and 1% Penicillin-Streptomycin solution (ThermoFisher, USA). The cells were incubated at 37°C in a humidified 5% CO₂ atmosphere.

In vivo Tumorigenesis and Metastasis Assays

BALB/c-nude mice were obtained from the Laboratory Animal Center at Sun Yat-sen University, Guangzhou, China. All mice were housed under specific pathogen-free (SPF) conditions. In the subcutaneous xenograft model, 6×10^6 HN6 cells were injected into the dorsal subcutaneous region of 5-week-old male BALB/c nude mice. For orthotopic xenograft: 5×10^5 HN6 cells were inoculated into the submucosa of the tongue of 5-week-old BALB/c nude mice according to previous reports.¹⁶

Vector Construction and Cell Transfection

We obtained circPRMT5-specific shRNA and overexpression lentiviruses, along with their respective negative controls (GenePharma, China). Cells were seeded into 6-well plates at a density of 5×10^4 cells per well. At around 30% confluence, the cells were infected with their respective lentiviral strains. After a 48-hour infection period, the stable transfection cell line was constructed by continuous screening with puromycin for 2 weeks.

Small interfering RNAs (siRNAs) targeting IGF2BP3, SERPINE1, and a negative control (NC) were procured from TsingKe Biotech (Beijing, China). The sequences of all siRNAs are detailed in [Supplemental Table S1](#). Following the manufacturer's protocol, siRNAs were transfected using the Lipofectamine 3000 kit (ThermoFisher, USA).

Assays of Cell Behavior in vitro

In the cell proliferation assay, SCC15 and HN6 cells were seeded into 96-well tissue-culture plates at a density of 1500 cells per well and incubated at 37°C for 24, 48, 72, and 96 hours, respectively. Cell viability was assessed using the Cell Counting Kit-8 (CCK-8, GOONIE, Japan) following the manufacturer's instructions.

In the colony formation experiment, cells were seeded at a density of 500 cells per well into 6-well plates with 2 mL of complete culture medium. After a 14-day incubation period, large colonies (comprising more than 100 cells per colony) were stained and manually counted.

In the wound healing assay, cells were seeded at a density of 8×10^5 cells per well in 6-well tissue-culture plates to achieve full confluence. Subsequently, a 1 mL pipette tip was employed to create a scratch. The detached cells were removed, and a serum-free medium was added. The width of the wound at 3–5 randomly selected sites was measured at 24 hours post-scratch, and the rate of wound closure was subsequently analyzed.

Migration and invasion assays utilized transwell filter chambers with 8.0 µm pores (Falcon, Corning, NY), without or with Matrigel (Corning, NY), as per the manufacturer's guidelines. Migrated cells were fixed, stained, and manually counted under a light microscope.

Quantitative Real-Time PCR (qRT-PCR)

Total RNA from human saliva exosomes was extracted using the TRIzol[®] reagent (ThermoFisher, USA) according to the manufacturer's protocols. For SCC15 and HN6 cells, as well as HNSCC tissues, total RNA was extracted using the RNA

Quick Purification Kit (ESscience, China). RNA reverse transcription (RT) was performed with the HiScript III RT SuperMix for qPCR (Vazyme, Nanjing, China). Subsequently, quantitative PCR (qPCR) was conducted using the ChamQ Universal SYBR qPCR Master Mix (Vazyme, China) on the QuantStudio™ Real-Time PCR System (ThermoFisher, USA). The corresponding primer sequences are detailed in [Supplemental Table S2](#).

Western Blot

Total protein extracted from SCC15 and HN6 cells was isolated using Radio Immunoprecipitation Assay (RIPA) lysis buffer (CWbio, China). After electrophoresis, membrane transfer, blocking, and overnight incubation of the primary antibody at 4°C, followed by a 1-hour incubation with secondary antibodies at room temperature, protein bands were detected using a Bio-Rad ChemiDoc XRS system (Bio-Rad, USA). Detailed information regarding the primary and secondary antibodies is provided in [Supplementary Table S3](#).

Fluorescence in Situ Hybridization (FISH) and Immunofluorescence (IF)

To assess the co-localization of circPRMT5 with the specified proteins, SCC15 and HN6 cells were subjected to fixation, permeabilization, and pre-hybridization. Following these preparatory steps, hybridization was conducted using Cy3-conjugated circPRMT5 probes at 37°C in the dark overnight. Post-hybridization, the cells were rinsed with SSC buffer at 42°C. Subsequently, the cells were incubated with a blocking buffer (PBST containing 5% bovine serum albumin) for 30 minutes at room temperature. Subsequently, the cells were incubated with a primary antibody at a 1:200 dilution for 1 hour at room temperature. This was followed by incubation with CoraLite488-conjugated secondary antibodies (1:200 dilution; Proteintech, USA) and DAPI (Servicebio, China) for 30 minutes. Imaging was performed using a Zeiss LSM 980 microscope equipped with Airyscan 2 technology (Zeiss, Germany).

circPRMT5 probe:

AAGGGTACCC GCATCCAGAA CTTGAGGAGC CGGAAGATGA

RNA Immunoprecipitation (RIP) Analysis

RIP analysis was conducted using the RNA Immunoprecipitation Kit (Genesee Biotech, China) following the manufacturer's instructions. SCC15 and HN6 cells were lysed in RIP buffer, and the resulting cell lysates were collected. Magnetic beads were conjugated with either IGF2BP3 antibody (anti-IGF2BP3, Proteintech, USA) or immunoglobulin G antibody (anti-IgG, Cell Signaling Technology, USA). After several washes, the precipitated RNA underwent qRT-PCR analysis. The corresponding primer sequences are detailed in [Supplemental Table S4](#).

Immunohistochemistry (IHC)

IHC was performed with primary antibodies targeting IGF2BP3, SERPINE1, or Ki67 (all at 1:250 dilution, ProteinTech, China), or Pan-cytokeratin (1:3000 dilution, ProteinTech, China). The proportion of Ki67-positive cells was quantified, and statistical analyses were performed to evaluate differences. Each sample for IGF2BP3 and SERPINE1 was assessed using a proportion score (1–4) for positively stained cells and an intensity score (1–3) for staining intensity. The staining index was calculated by multiplying the proportion score with the intensity score, and subsequent statistical analysis was conducted to assess differences.

Protein and RNA Stability Assays

Protein stability was evaluated in SCC15 and HN6 cells infected with lentivirus by treating them with cycloheximide (CHX, 100 µg/mL; MCE, USA) at multiple specific points in time. IGF2BP3 expression levels were quantified via Western blot and normalized to β-actin. For RNA stability assays, SCC15 and HN6 cells were exposed to actinomycin D (5 µg/mL) at multiple specific points in time. Total RNA was isolated and analyzed using qRT-PCR, with the relative levels of circPRMT5, PRMT5, and SERPINE1 quantified and normalized to GAPDH.

Isolation and Identification of Salivary Exosomes

Saliva samples (5 mL) were collected from healthy donors and patients with HNSCC and subjected to centrifugation at $3000\times g$ and 4°C (Thermo Scientific, USA) for 30 minutes. The supernatant was subsequently collected and further centrifuged at $160,000\times g$ for 1.5 hours (Beckman coulter, USA) to isolate the saliva exosome precipitate. Western blotting, transmission electron microscopy (TEM) (Hitachi, Japan), and the NanoSight NS300 (Malvern Panalytical, UK) were used to identify exosomes.

Data Acquisition

The RNA-Seq data for SCC15 was procured from Metware (China), and the raw data has been uploaded to the Gene Expression Omnibus (GEO) (GSE277717). Additionally, TCGA and CPTAC datasets for HNSCC were retrieved from the UALCAN portal (<https://ualcan.path.uab.edu/>, up to July 30, 2024).^{17,18}

Statistical Analysis

Statistical analyses were conducted utilizing SPSS software version 27.0 (SPSS Inc., USA) and GraphPad Prism version 9.0 (GraphPad Software, USA). Data are presented as mean \pm standard deviation (SD) unless stated otherwise. The Student's *t*-test and one-way analysis of variance (ANOVA) were used to compare continuous variables between two or more groups. Differences in mRNA and circRNA expression between the two groups were evaluated using an unpaired *t*-test for independent samples and a paired *t*-test for matched samples. The association between circPRMT5 expression and clinicopathological characteristics was assessed using Pearson's Chi-Square test. Fisher's exact test was employed to evaluate lymph node metastasis in orthotopic xenograft models. Receiver operating characteristic (ROC) curves were used to determine the specificity and sensitivity of circPRMT5, and the area under the curve (AUC) was calculated. The relationship between IGF2BP3 and SERPINE1 was examined through Pearson's correlation analysis. $p < 0.05$ was deemed to indicate statistical significance.

Results

circPRMT5 Was Overexpressed in HNSCC and Enhanced the Proliferation, Migration, and Invasion of HNSCC in vitro

To assess the expression levels of circPRMT5 in HNSCC tissues, qRT-PCR was employed to analyze both HNSCC tissue samples and their corresponding adjacent non-tumor tissues ($n=53$). The results revealed a notable increase in circPRMT5 expression in HNSCC tissues relative to adjacent non-tumor tissues (Figure 1A and B, $p < 0.001$). Through the analysis of clinical data from patients with HNSCC, it was observed that circPRMT5 expression exhibited a significant correlation with both the T stage ($p=0.037$) and cervical lymph node metastasis ($p=0.006$) (Table 1). The ring structure of circPRMT5 was confirmed through Sanger sequencing, Actinomycin D treatment and gel electrophoresis (Figure 1C–E). Furthermore, circPRMT5 expression levels were significantly higher in most HNSCC cell lines compared to a normal oral keratinocyte (NOK) cell line (Figure 1F). Consequently, the SCC15 and HN6 cell lines were chosen for subsequent functional experiments. To elucidate the potential role of circPRMT5 in the biological processes of HNSCC, we generated stable cell lines with either overexpression or knockdown of circPRMT5 in SCC15 and HN6 cells through lentiviral transfection. The application of circPRMT5 shRNA resulted in a significant reduction of circPRMT5 levels, while overexpression vectors markedly increased circPRMT5 expression in HNSCC cells, without altering PRMT5 mRNA levels (Figure 1G and H). CCK8 assays and colony formation assays demonstrated that circPRMT5 overexpression significantly enhanced the proliferation of HNSCC cells (Figure 1I and J). Metastasis, a hallmark of cancer, greatly affects the prognosis of HNSCC patients. In this study, we examined the influence of circPRMT5 on the migratory and invasive capabilities of HNSCC cells. Our findings indicated that overexpression of circPRMT5 significantly enhanced the migratory capacity and invasiveness of HNSCC cells (Figure 1K and L). Conversely, the knockdown of circPRMT5 markedly suppressed the proliferation (Figure 1M and N), migration (Figure 1O and P), and invasion (Figure 1P) of SCC15 and HN6 cells. Consequently, our findings indicate that circPRMT5 is upregulated in HNSCC and promotes the proliferation, migration, and invasion of HNSCC cells in vitro.

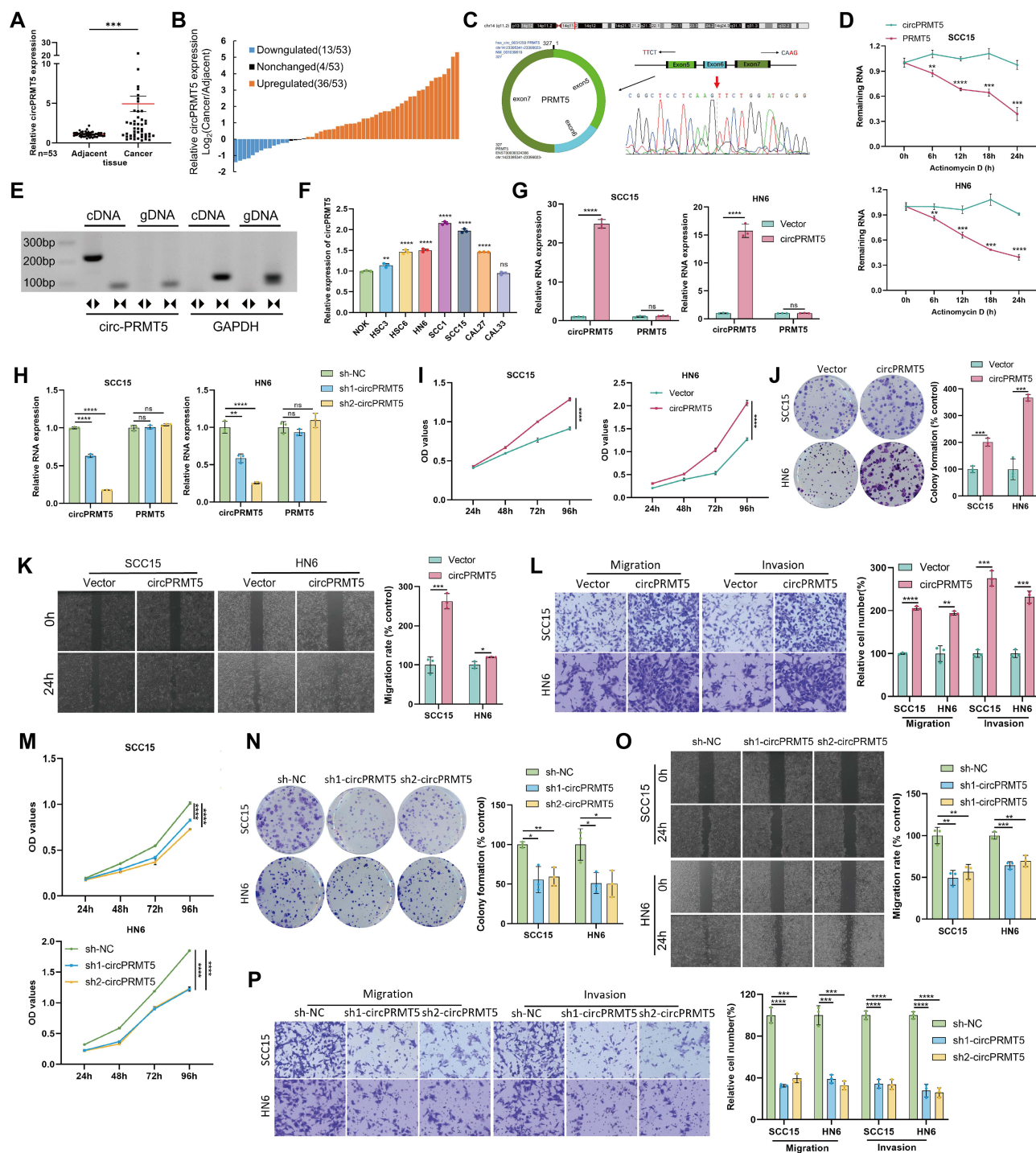


Figure 1 Identification, characterization, and functions of circPRMT5 in HNSCC. (A) qRT-PCR analysis of circPRMT5 expression in 53 pairs of HNSCC tissues and matched adjacent noncancerous tissues. n=53. Data were presented as mean ± SEM. (B) An increase in circPRMT5 expression is observed in 67.9% of the HNSCC patients. n=53. (C) Sanger sequencing verified the sequence of circPRMT5. (D) The expression level of circPRMT5 and PRMT5 mRNA in the condition of Actinomycin D treatment. (E) Agarose gel electrophoresis assay verified the existence of circPRMT5 in HNSCC cells. (F) qRT-PCR analysis of circPRMT5 expression in NOK and HNSCC cells. (G and H) qRT-PCR analysis of circPRMT5 and PRMT5 mRNA in HNSCC cells treated with two shRNAs or circPRMT5 overexpression lentivirus. (I and J) The proliferation of HNSCC cells transfected with circPRMT5 overexpression lentivirus evaluated by CCK-8 (I) and plate colony formation (J). (K) The migration ability of HNSCC cells following circPRMT5 overexpression was assessed using a wound healing assay. (L) Transwell assays assessed the migration and invasion capabilities of HNSCC cells following circPRMT5 overexpression. (M and N) The proliferation of HNSCC cells transfected with circPRMT5 shRNA lentivirus was evaluated by CCK-8 (M) and plate colony formation (N). (O) The migration ability of HNSCC cells following circPRMT5 knockdown was assessed using a wound healing assay. (P) Transwell assays assessed the migration and invasion capabilities of HNSCC cells following circPRMT5 knockdown. *p < 0.05, **p < 0.01, ***p < 0.001, ****p < 0.0001. **Abbreviation:** ns, not significant.

Table 1 Relationship Between circPRMT5 Expression in Tissues of HNSCC Patients and Their Clinicopathological Parameters

Characteristics	No. of Cases	circPRMT5 Expression		P value	χ^2
		Low (%)	High (%)		
Age				0.565	0.013
<50	31	15	16		
≥50	22	11	11		
Gender				0.531	0.058
Male	40	20	20		
Female	13	6	7		
Areca catechu history				0.582	0.008
Yes	16	8	8		
No	37	18	19		
Smoking history				0.560	0.016
Yes	29	14	15		
No	24	12	12		
T-primary tumor				0.037	4.246
Tis+T1+T2	23	15	8		
T3+T4	30	11	19		
N-regional lymph node				0.006	7.815
Yes	13	2	11		
No	40	24	16		
Histological grade				0.057	3.592
Well	41	23	18		
Moderately+Poorly	12	3	9		

Abbreviations: HNSCC, Head and neck squamous cell carcinoma; OSCC, Oral squamous cell carcinoma; CircRNA, Circular RNA; MiRNA, MicroRNA; ATCC, American Type Culture Collection; CCK-8, Cell Counting Kit-8; H&E, Hematoxylin and eosin staining; IHC, Immunohistochemistry assay; PCK, Pan-cytokeratin; TCGA, The Cancer Genome Atlas; CPTAC, Clinical Proteomic Tumor Analysis Consortium; GEO, Gene Expression Omnibus; RBP, RNA binding protein; IGF2BP3, Insulin-like growth factor 3 mRNA-binding protein 2; SERPINE1, Serine protease inhibitor clade E member 1; PAI-1, Plasminogen Activator Inhibitor 1; qRT-PCR, Quantitative real-time polymerase chain reaction; FISH, Fluorescence in situ hybridization; EMT, Epithelial-mesenchymal transition; RIP, RNA immunoprecipitation; ROC, Receiver Operating Characteristic.

circPRMT5 Promotes the Proliferation and Metastasis of HNSCC Cells in vivo

We examined circPRMT5's role in cancer progression using a xenograft model. sh1-circPRMT5-HN6, sh2-circPRMT5-HN6, or sh-NC-HN6 cells were subcutaneously implanted into the dorsal region of BALB/c nude mice and monitored for 1–4 weeks. The sh1-circPRMT5 and sh2-circPRMT5 groups showed significantly reduced tumor volumes and weights compared to the sh-NC group (Figure 2A–C). There was no significant difference in body weight among the three groups (Supplementary Figure S1A). Tumor cell proliferation was identified via Ki-67 immunostaining. The sh-NC group exhibited a significantly higher number of Ki-67-positive (Ki67+) cells compared to the sh1-circPRMT5 and sh2-circPRMT5 groups (Figure 2D and E). Furthermore, the liver, kidney, and lung tissues of the three groups of nude mice exhibited no abnormalities (Supplementary Figure S1B).

We examined the effect of circPRMT5 on cervical lymph node metastasis using an orthotopic xenograft model, implanting circPRMT5-HN6 or Vector-HN6 cells into the tongues of BALB/c nude mice. The overexpression of circPRMT5 was observed to enhance the growth of primary tumors (Figure 2F–H) and significantly reduced body weight in the nude mice by the end of the experiment (Supplementary Figure S1C). Cervical lymph node metastasis was evaluated using hematoxylin and eosin (H&E) staining and pan-cytokeratin (PCK) immunohistochemistry. The findings indicated that circPRMT5 overexpression significantly increased the incidence of cervical lymph node metastasis compared to the Vector group (Figure 2I and J). Notably, no distant metastasis was observed (Supplementary Figure S1D). These findings indicate that circPRMT5 promotes tumorigenesis and cervical lymph node metastasis in HNSCC in vivo.

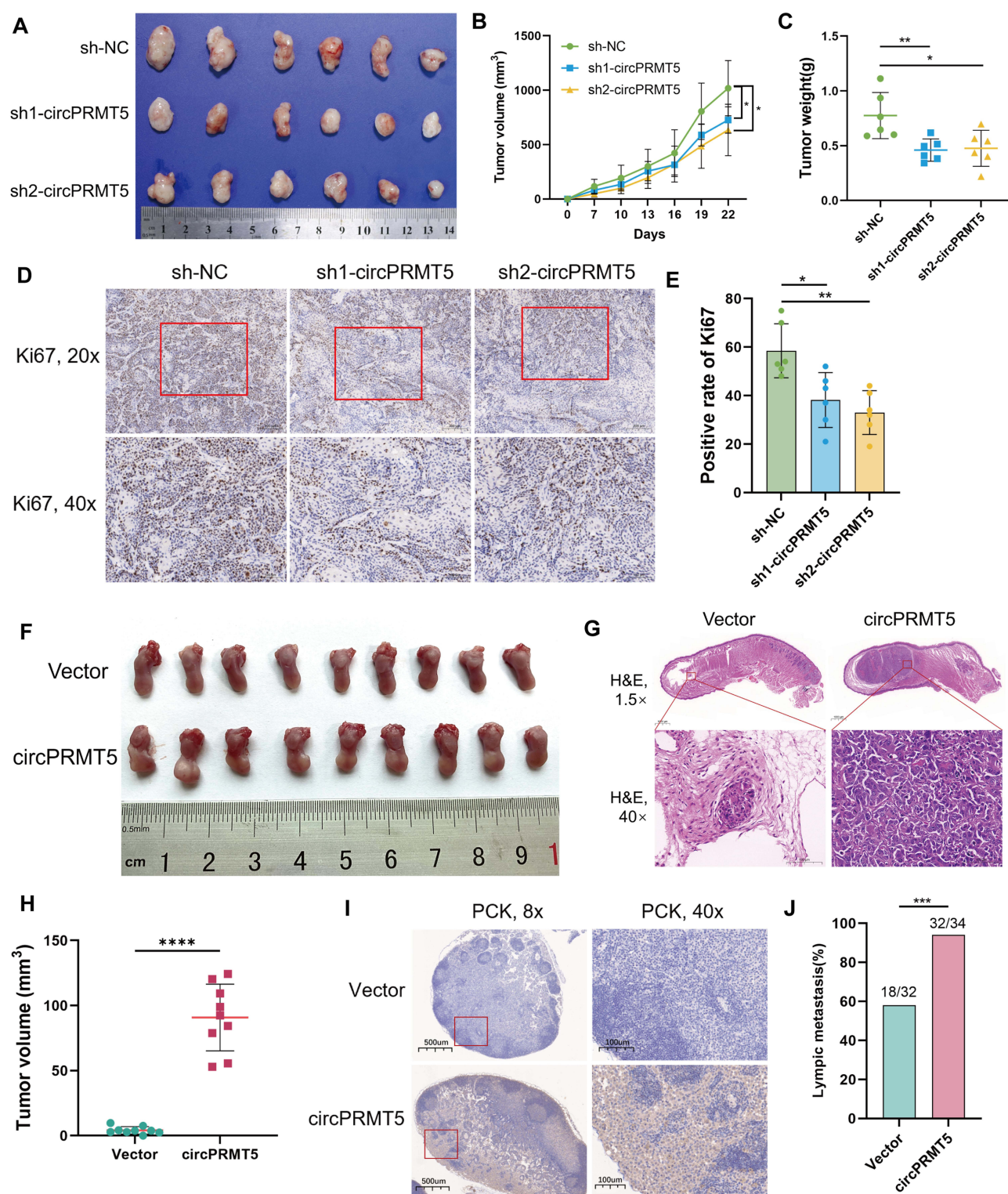


Figure 2 circPRMT5 promoted proliferation and metastasis of HNSCC in vivo. (A–C) The appearance (A), volume change quantification (B), and tumor weight (C) of HNS6 xenografts transfected with sh-NC (n=6), sh1-circPRMT5 (n=6), and sh2-circPRMT5 (n=6) in BALB/c nude mice. (D and E) Representative IHC staining of Ki-67 (D) and quantification of Ki-67⁺ cells (E) in sh-NC, sh1-circPRMT5, and sh2-circPRMT5 groups. (F) The appearance of HNS6 orthotopic tumors. (G) Representative H&E staining of the longitudinal section of tongues. Scale bar 1000μm, 100μm. (H) Quantification of orthotopic tumor volumes in Vector (n=9) and circPRMT5 (n=9) groups in orthotopic xenografts. (I) Representative IHC staining of metastatic tumor cells in cervical lymph nodes from Vector and circPRMT5 groups using anti-pan-cytokeratin (PCK). Scale bar 500μm, 100μm. (J) Statistical analysis of cervical lymph node metastasis rates between Vector and circPRMT5 groups. **p*<0.05, ***p*<0.01, ****p*<0.001, *****p*<0.0001.

circPRMT5 Binds to and Stabilizes the IGF2BP3 Protein to Promote the Proliferation, Migration and Invasion of HNSCC Cells

Using the RBPsuite (<http://www.csbio.sjtu.edu.cn/bioinf/RBPsuite/>) and circinteractome (<https://circinteractome.nia.nih.gov/>) databases, we predicted RNA-binding proteins (RBPs) associated with circPRMT5 and identified five common RBPs (Figure 3A). Among these, insulin-like growth factor 2 mRNA-binding protein 3 (IGF2BP3) was predicted to bind both the junction and flanking regions of circPRMT5, with its enrichment degree for circPRMT5 being significantly higher than that of IgG (Supplementary Figure S2A and B). Consequently, IGF2BP3 was selected as a candidate protein for subsequent mechanistic studies. RIP assays were conducted to confirm the interaction between IGF2BP3 and circPRMT5 in HNSCC. The findings indicated that inhibiting circPRMT5 reduces its binding to IGF2BP3, implying that circPRMT5 expression levels influence its interaction with IGF2BP3 (Figure 3B, $p < 0.0001$, $p < 0.001$). Immunofluorescence and FISH assays verified the co-localization of circPRMT5 and IGF2BP3 in HNSCC cells (Figure 3C). Subsequent analyses demonstrated that overexpression of circPRMT5 elevated the protein levels of IGF2BP3, whereas knockdown of circPRMT5 resulted in a reduction of IGF2BP3 protein levels (Figure 3D). Following the application of cycloheximide (CHX) to HNSCC cells for varying durations, protein extracts were analyzed, revealing that circPRMT5 overexpression markedly inhibited the degradation of IGF2BP3 protein (Figure 3E). These findings suggest that circPRMT5 may bind to and stabilize IGF2BP3.

We conducted a comprehensive database search to elucidate the expression pattern of IGF2BP3 in HNSCC. Analysis of data from The Cancer Genome Atlas (TCGA) and Clinical Proteomic Tumor Analysis Consortium (CPTAC) databases indicated significantly elevated mRNA and protein levels of IGF2BP3 in HNSCC compared to normal tissues (Figure 3F and G, $p < 0.0001$). Furthermore, examination of 53 paired tissue samples demonstrated that IGF2BP3 expression was markedly higher in HNSCC tissues relative to adjacent non-cancerous tissues (Figure 3H and I, $p < 0.0001$). Additionally, we constructed a small interfering RNA (siRNA) targeting IGF2BP3 and confirmed the knockdown efficiency (Supplementary Figure S3A and B). Our results indicated that IGF2BP3 knockdown did not alter circPRMT5 RNA levels (Supplementary Figure S3A). Silencing IGF2BP3 markedly inhibited the proliferation, migration, and invasion of HNSCC cells (Supplementary Figure S3C–E). Subsequently, we designed and validated a rescue experiment to confirm these findings (Figure 3J). Rescue experiments demonstrated that the knockdown of IGF2BP3 could counteract the increased cell proliferation, invasion, and migration induced by circPRMT5 overexpression (Figure 3K–M). These findings indicate that IGF2BP3 is essential for circPRMT5-mediated promotion of proliferation, migration, and invasion in HNSCC.

CircPRMT5 Interacts With IGF2BP3 to Modulate SERPINE1 mRNA Stability

To clarify how circPRMT5-IGF2BP3 influenced the proliferation and metastasis of HNSCC, we performed RNA sequencing (RNA-seq) on SCC15 cells transfected with sh2-circPRMT5, si1-IGF2BP3, and their respective controls (Figure 4A and B). Analysis of RNA-seq data identified 14 differentially expressed candidate genes common to both experimental groups (Figure 4C). Among these, serpin family E member 1 (SERPINE1) emerged as the most significantly differentially expressed gene. Consequently, we identified SERPINE1 as a potential target of the circPRMT5-IGF2BP3 regulatory axis (Figure 4D). Subsequently, we assessed the expression of SERPINE1 in HNSCC cells by modulating the levels of circPRMT5 and IGF2BP3 through overexpression and inhibition techniques. Notably, overexpression of circPRMT5 significantly upregulated SERPINE1 mRNA and protein levels, while its knockdown reduced these levels (Figure 4E, F and H). Similarly, the knockdown of IGF2BP3 significantly decreased the mRNA and protein expression of SERPINE1 (Figure 4G and I). Given IGF2BP3's role as a key RNA-binding protein affecting mRNA stability, we hypothesize that the circPRMT5-IGF2BP3 complex may regulate SERPINE1 mRNA expression by modulating its stability. RIP experiments showed a notable decrease in IGF2BP3 protein binding to SERPINE1 mRNA after circPRMT5 knockdown (Figure 4J). Subsequently, an mRNA decay assay for SERPINE1 was conducted. Overexpression of circPRMT5 resulted in a deceleration of SERPINE1 mRNA degradation. However, inhibition of IGF2BP3 in circPRMT5-overexpressing cell lines notably reversed this deceleration (Figure 4K, $p < 0.01$). Collectively, these findings suggest that circPRMT5 stabilizes SERPINE1 mRNA by interacting with IGF2BP3, leading to increased SERPINE1 expression.

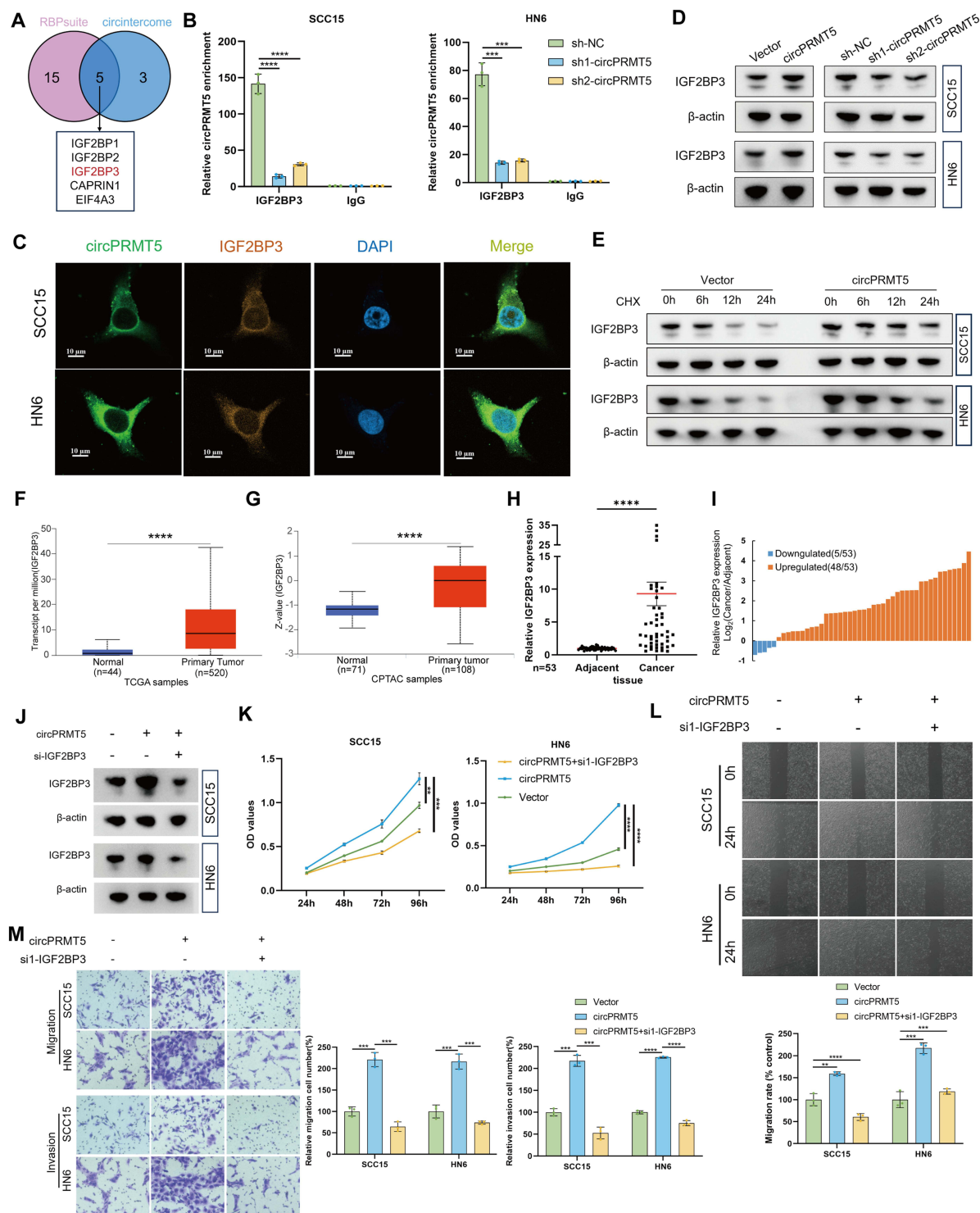


Figure 3 circPRMT5 interacted with and stabilized IGF2BP3, thereby enhancing the proliferation and metastasis of HNSCC. **(A)** Venn diagram of predicted circPRMT5 binding proteins in the circintercome database and the RBPsuite database. **(B)** The enrichment of circPRMT5 pulled down by IGF2BP3 protein in HNSCC cells with or without knockdown the circPRMT5 was analyzed by qRT-PCR. **(C)** IF and FISH images represented the colocalization of circPRMT5 and IGF2BP3 in HNSCC cells. **(D)** Western Blots (WB) showed the change of IGF2BP3 expression after overexpression and knockdown of circPRMT5. **(E)** CHX assays combined with WB were used to evaluate the stability of IGF2BP3 protein in HNSCC cells following circPRMT5 overexpression. **(F)** IGF2BP3 mRNA expression from the TCGA database. **(G)** IGF2BP3 protein levels in HNSCC from the CPTAC database. **(H)** qRT-PCR analysis of IGF2BP3 expression in 53 pairs of HNSCC tissues and matched adjacent noncancerous tissues. n=53. Data are presented as mean±SEM. **(I)** An increase in IGF2BP3 expression was observed in 90.6% of the HNSCC patients. n=53. **(J)** WB verified the expression of IGF2BP3 in the rescue experiment. **(K)** CCK8 assays revealed changes in the proliferation of HNSCC cells during circPRMT5 overexpression or combined IGF2BP3 knockdown. **(L)** Representative images and quantitative analysis of wound healing assays showed that overexpression of circPRMT5 or combined with IGF2BP3 knockdown induced changes in HNSCC cell migration. **(M)** Representative images and quantitative analysis of transwell assays demonstrated that circPRMT5 overexpression, either alone or in combination with IGF2BP3 knockdown, affected HNSCC cell migration and invasion. ** $p < 0.01$, *** $p < 0.001$, **** $p < 0.0001$.

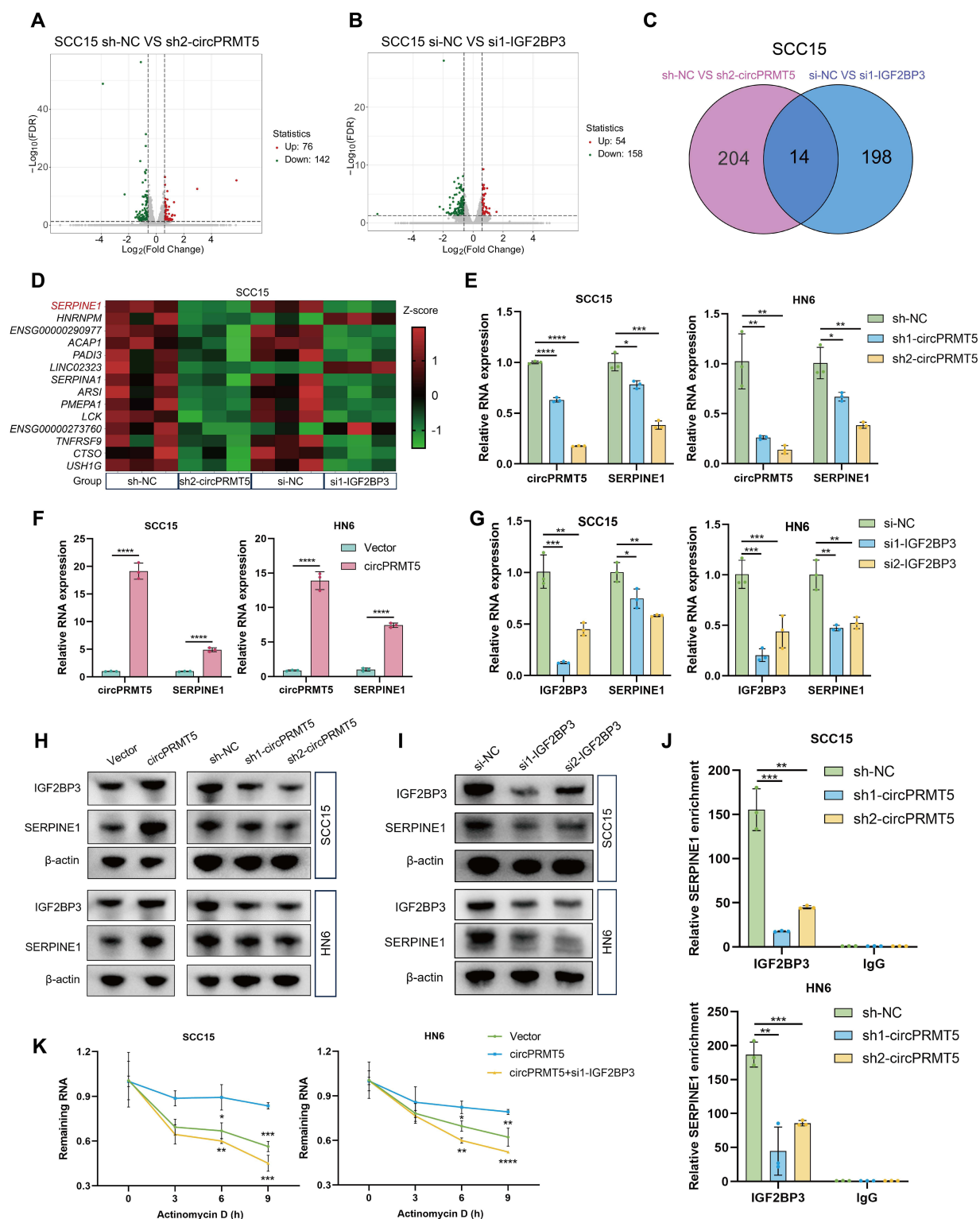


Figure 4 circPRMT5/IGF2BP3 stabilized the mRNA of SERPINE1. **(A)** A volcanic map of differential genes was generated following transcriptome sequencing after circPRMT5 knockdown. **(B)** A volcanic map of differential genes identified post-transcriptome sequencing following IGF2BP3 knockdown. **(C)** A venn diagram of intersection of differential genes of sh-NC VS sh2-circPRMT5 and si-NC VS si1-IGF2BP3. **(D)** A heat map of differential genes identified in the Venn diagram. **(E)** and **(F)** The mRNA levels of SERPINE1 and circPRMT5 when circPRMT5 was overexpressed or knockdown were tested by qRT-PCR. **(G)** The mRNA levels of SERPINE1 when IGF2BP3 was knockdown were tested by qRT-PCR. **(H)** The protein levels of SERPINE1 and IGF2BP3 when circPRMT5 was overexpressed or knockdown was tested by Western blot. **(I)** The protein levels of SERPINE1 and IGF2BP3 when IGF2BP3 was knockdown were tested by Western blot. **(J)** The enrichment of SERPINE1 pulled down by IGF2BP3 protein in HNSCC cells with or without knockdown of the circPRMT5 was analyzed by qRT-PCR. **(K)** The actinomycin D assay demonstrated the stability of SERPINE1 mRNA in HNSCC cells when circPRMT5 overexpression, either alone or in combination with IGF2BP3 knockdown at the specified time point. * $p < 0.05$, ** $p < 0.01$, *** $p < 0.001$, **** $p < 0.0001$.

CircPRMT5 Promotes the Proliferation and Invasion Ability of HNSCC Cells in a SERPINE1-dependent Manner

We performed an extensive database search to clarify the expression pattern of SERPINE1 in HNSCC. Analysis of TCGA and CPTAC data indicated significantly higher mRNA and protein expression levels of SERPINE1 in HNSCC compared to normal controls (Figure 5A and B, $p < 0.0001$). Further examination of 53 HNSCC tissues and their corresponding adjacent non-tumorous tissues demonstrated that SERPINE1 expression was markedly higher in HNSCC tissues (Figure 5C and D, $p < 0.0001$). Subsequently, immunohistochemical staining and scoring were performed on HNSCC tissue and subcutaneous tumor tissue samples of nude mice to determine the expression levels of IGF2BP3 and SERPINE1 proteins. Our results showed that IGF2BP3 protein was significantly correlated with SERPINE1 protein both in tumor tissues of HNSCC patients (Figure 5E, G, $r = 0.6570$, $p < 0.0001$) and subcutaneous tumors of nude mice (Figure 5F, H, $r = 0.5097$, $p < 0.05$). Furthermore, we synthesized small interfering RNA targeting SERPINE1 and confirmed the knockdown efficiency (Supplementary Figure S4A). Our results indicated that SERPINE1 knockdown did not influence the RNA levels of circPRMT5 and IGF2BP3, nor the protein level of IGF2BP3 (Supplementary Figure S4A and B). The significant reduction of SERPINE1 markedly inhibited the proliferation, migration, and invasion of HNSCC cells (Supplementary Figure S4C–E). Subsequently, we performed a rescue experiment. Western blot analysis demonstrated that IGF2BP3 knockdown could mitigate the upregulation of SERPINE1 induced by circPRMT5 overexpression. However, the down-regulation of SERPINE1 did not mitigate the up-regulation of IGF2BP3 induced by the overexpression of circPRMT5 (Figure 5I). Additionally, cell function assays demonstrated that the knockdown of SERPINE1 attenuated the circPRMT5 overexpression-induced enhancement of cell proliferation, invasion, and migration (Figure 5J–L). In summary, our findings indicate that SERPINE1 is a target of the circPRMT5/IGF2BP3 axis and may play a crucial role in the circPRMT5-mediated enhancement of HNSCC cell proliferation and metastasis.

CircPRMT5 Is Upregulated in the Salivary Exosomes of Patients with HNSCC and Associated with Lymph Node Metastasis and Advanced T-Stage

Given the established correlation between tumor location and saliva in patients with HNSCC, we aimed to investigate the expression of circPRMT5 in salivary exosomes. Salivary exosomes were extracted and characterized from both HNSCC patients and healthy donors (Figure 6A). The purified exosomes exhibit typical characteristics, including a cup-shaped morphology, the expression of the labeled proteins CD63, CD81, and TSG101, and diameters ranging from 40 to 160 nm (Figure 6B–D). These findings confirm the successful isolation of exosomes from the saliva of HNSCC patients. Subsequently, the expression of circPRMT5 in saliva exosomes from 72 HNSCC patients and 29 healthy donors was analyzed. The results demonstrated that the expression of circPRMT5 in the saliva exosomes of HNSCC patients was significantly elevated compared to healthy donors (Figure 6E, $p < 0.01$). We then conducted a receiver operating characteristic (ROC) curve analysis to assess the potential of circPRMT5 expression levels in salivary exosomes as a biomarker for distinguishing HNSCC patients from healthy individuals. The analysis showed an area under the curve (AUC) of 0.9133 ($p < 0.0001$) (Figure 6F), indicating that circPRMT5 in salivary exosomes possesses high diagnostic accuracy for HNSCC. These findings suggest significant clinical application potential for circPRMT5 as a diagnostic tool in HNSCC. Further statistical analysis indicated that patients with elevated circPRMT5 expression were more prone to cervical lymph node metastasis and advanced clinical stages (Figure 6G and H, $p < 0.05$). In addition, saliva samples were obtained from a subset of patients one month following tumor resection for subsequent analysis. The results indicated a significant down-regulation in the expression of circPRMT5 in post-resection saliva compared to pre-resection levels (Figure 6I, $p < 0.0001$). These findings substantiate the potential of circPRMT5 as a noninvasive diagnostic and prognostic marker, underscoring its significant clinical utility.

Discussion

An expanding corpus of research has investigated the biogenesis, characterization, and function of circular RNAs, revealing their aberrant behavior in various cancers and suggesting their potential role in regulating cancer progression.^{9,12,19,20} Nevertheless, circRNAs with diagnostic value in saliva for HNSCC remain scarce. The mechanisms by which circRNAs affect HNSCC proliferation and metastasis need further elucidation. Numerous studies have

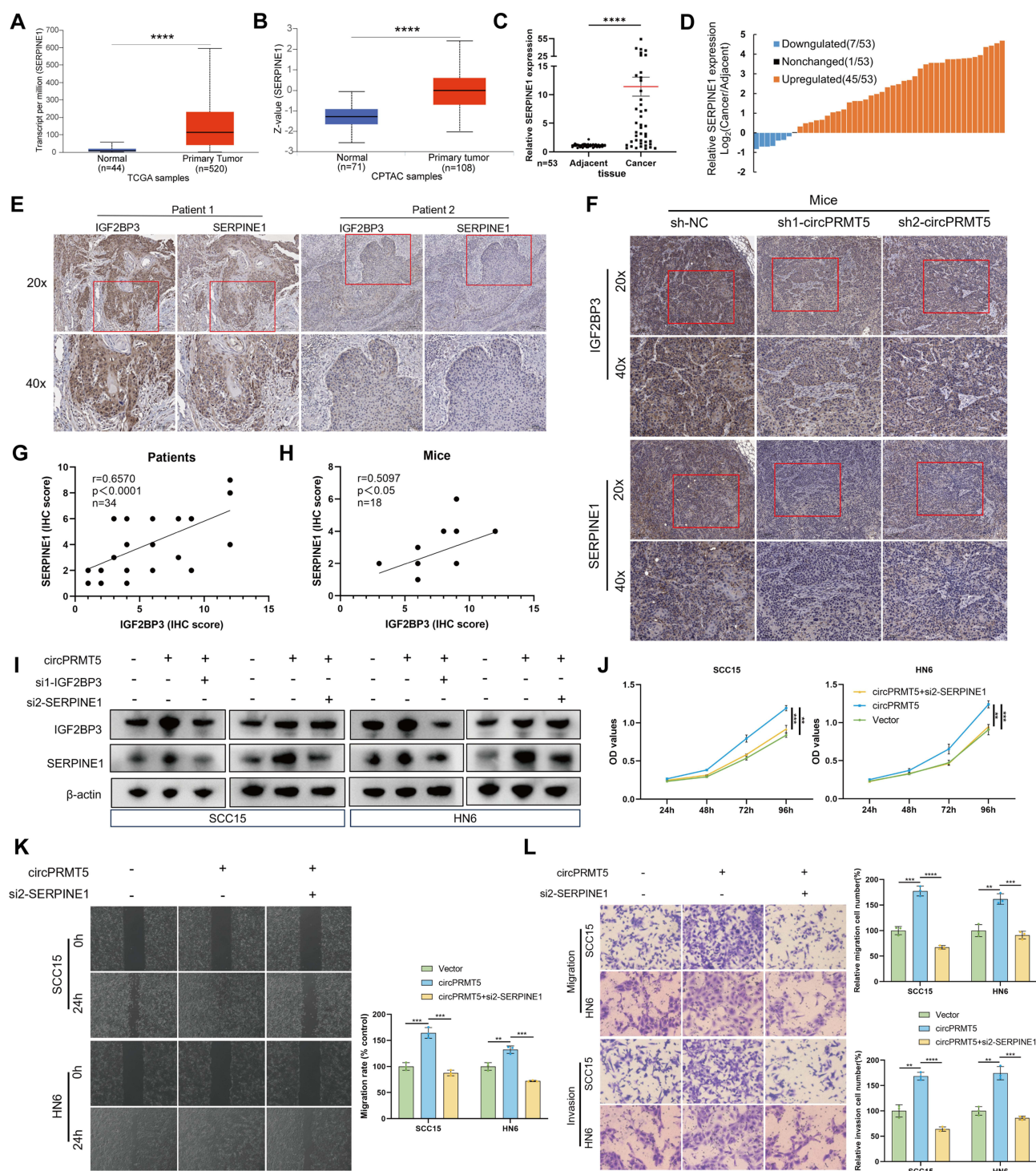


Figure 5 The promotion effect of circPRMT5/IGF2BP3 on HNSCC required the participation of SERPINE1. **(A)** The mRNA expression of SERPINE1 in HNSCC in TCGA database. **(B)** The protein level of SERPINE1 in HNSCC in the CPTAC database. **(C)** qRT-PCR analysis of SERPINE1 expression in 53 pairs of HNSCC tissues and matched adjacent noncancerous tissues. $n=53$. Data are presented as mean \pm SEM. **(D)** An increase in SERPINE1 expression is observed in 84.9% of the HNSCC patients. $n=53$. **(E)** The protein levels of IGF2BP3 and SERPINE1 in HNSCC tissues were measured via IHC. **(F)** The protein levels of IGF2BP3 and SERPINE1 in subcutaneous tumors of nude mice were measured via IHC. **(G)** Correlation analysis of IGF2BP3 and SERPINE1 expression in HNSCC. $r=0.6570$, $p<0.0001$. **(H)** Correlation analysis of IGF2BP3 and SERPINE1 expression in subcutaneous tumors of nude mice. $r=0.5097$, $p<0.05$. **(I)** WB verified the expression of IGF2BP3 and SERPINE1 in the IGF2BP3 rescue experiment. **(J)** CCK8 assays revealed changes in the proliferation of HNSCC cells during circPRMT5 overexpression or combined SERPINE1 knockdown. **(K)** Representative images and quantitative analysis of wound healing assays showed that overexpression of circPRMT5 or combined with SERPINE1 knockdown induced changes in HNSCC cell migration. **(L)** Representative images and quantitative analysis of transwell assays demonstrated that circPRMT5 overexpression, either alone or in combination with SERPINE1 knockdown, affected HNSCC cell migration and invasion. ** $p<0.01$, *** $p<0.001$, **** $p<0.0001$.

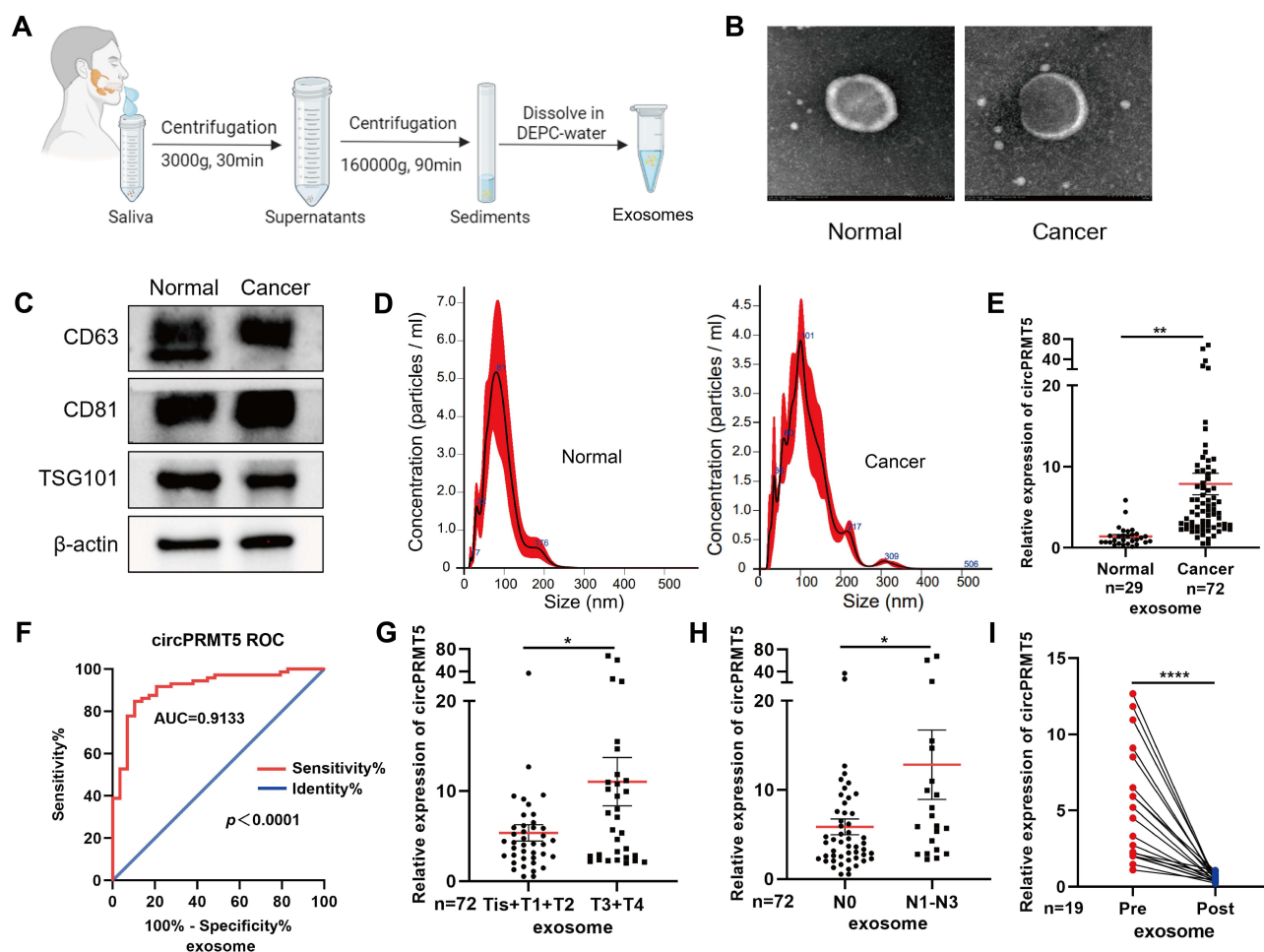


Figure 6 circPRMT5 was up-regulated in the saliva of HNSCC patients. **(A)** Schematic diagram of saliva exosome extraction method. **(B)** Transmission electron microscopy identified the exosomes. **(C)** Exosome marker levels (CD63, CD81, TSG101) in purified exosomes were detected using WB. **(D)** The NanoSight particle tracking analysis was used to determine the size distributions and quantities of exosomes. **(E)** The level of circPRMT5 in exosomes from the saliva of HNSCC patients was compared to that of healthy donors. Data were presented as mean±SEM. **(F)** ROC curve analysis of the accuracy of salivary exosome circPRMT5 in the diagnosis of HNSCC. AUC=0.9133, $p<0.0001$. **(G)** The expression of circPRMT5 in the saliva of HNSCC patients varied with different T stages. Data were presented as mean±SEM. **(H)** circPRMT5 expression in the saliva of HNSCC patients varied with different N stages. Data were presented as mean±SEM. **(I)** Postoperative circPRMT5 levels in salivary exosomes of HNSCC patients were compared with the corresponding preoperative levels. * $p<0.05$, ** $p<0.01$, *** $p<0.0001$.

demonstrated that circPRMT5 significantly promotes tumor progression in bladder, lung, and liver cancers.^{14,15,21} However, current research predominantly investigates the interaction between circPRMT5 and miRNA, with limited exploration of its interaction with RBPs.²² In this study, we elucidated a novel mechanism wherein the circPRMT5-IGF2BP3-SERPINE1 axis modulates the progression of HNSCC. Additionally, we identified the diagnostic potential of saliva-derived circPRMT5 in patients with HNSCC.

CircRNAs play essential biological roles by acting as miRNA sponges, modulating protein activity, or translating into proteins.²³ While the interactions between circPRMT5 and various miRNAs have been extensively investigated, the mechanisms underlying the binding between circPRMT5 and RNA-binding proteins (RBPs) remain largely unexplored, necessitating further comprehensive analysis.^{14,15,21,22} In this study, we predicted and experimentally validated the interaction between IGF2BP3 and circPRMT5. Multiple studies have demonstrated that IGF2BP3 is aberrantly expressed in various malignant tumors.^{24–26} IGF2BP3 overexpression enhances tumor cell proliferation, migration, invasion, and growth.^{27–29} Recent studies confirm that IGF2BP3 is significantly upregulated in oral squamous cell carcinoma (OSCC) tissues and is closely linked to poor prognosis and decreased overall survival in OSCC patients.^{30,31} Our research revealed a notable up-regulation of IGF2BP3 expression in HNSCC, and its knockdown markedly inhibited the proliferation, migration, and invasion capacities of HNSCC cells. Numerous studies have explored the mechanisms

underlying IGF2BP3 function. IGF2BP3 has been proven to enhance cancer cell proliferation by interacting with circARID1, forming the circARID1A-IGF2BP3-SLC7A5 RNA-protein complex.²⁵ Additionally, The IGF2BP3-regulated TMA7-UBA2-PI3K pathway has been identified as the primary mechanism through which TMA7 suppresses autophagy and promotes LSCC progression.³² Importantly, the presence of IGF2BP3 in OSCC is notably associated with epithelial-mesenchymal transition (EMT) markers, indicating its potential role in facilitating metastasis.³³ Interestingly, through RNA-seq and cross-analysis, we identified SERPINE1 as a novel downstream gene shared by circPRMT5 and IGF2BP3. Furthermore, our findings suggest that both circPRMT5 and IGF2BP3 contribute to the stabilization of SERPINE1 mRNA, thereby exerting a regulatory influence.

SERPINE1, also known as PAI-1, has been documented to exhibit elevated expression levels in various tumor types and to influence EMT. PAI-1 modulates the tumor microenvironment (TME) and regulates tumor cells migration and invasion.³⁴ Elevated levels of PAI-1 are significantly correlated with certain metastatic tumors and are associated with reduced overall survival and poorer prognosis.^{35–37} PAI-1 activates the AKT/ERK1/2 pathways by interacting with LRP1 directly, thereby enhancing EndoMT activity in lymphatic endothelial cells (LECs).³⁸ SERPINE1 is implicated in the partial induction of EMT, which is associated with a higher metastatic risk compared to full EMT induction in OSCC.^{39,40} Similarly, our study revealed that SERPINE1 expression is significantly up-regulated in HNSCC, promoting the proliferation, invasion, and migration of HNSCC cells. Notably, through RNA-seq, we have identified an innovative finding that SERPINE1 serves as a downstream target common to both circPRMT5 and IGF2BP3. The involvement of SERPINE1 is essential for the circPRMT5-IGF2BP3 axis in promoting HNSCC. However, the mechanisms or signaling pathways by which SERPINE1 enhances the proliferation and invasion of HNSCC cells warrant further investigation.

Liquid biopsies, involving minimally invasive tests using biological fluids like blood, saliva, and urine, have revolutionized cancer diagnosis and prognosis prediction.^{41,42} Most cells actively secrete exosomes, lipid bilayer vesicles with diameters ranging from 40 to 160 nm, and they circulate in body fluid.⁴³ Exosomes can reflect alterations in the physiological and pathological states of their parent cells.^{44,45} These findings indicate that analyzing circulating exosomes and their derivatives could offer new opportunities for cancer liquid biopsies, emphasizing their potential as biomarkers for cancer diagnosis, progression monitoring, and prognosis prediction.⁴² Numerous salivary or blood-derived miRNAs, including miR-23a, miR-9, miR-24-3p, and miR-21 have been identified as predictors of HNSCC or OSCC.^{46–49} However, there is limited literature on the role of saliva-derived circRNAs in diagnosing HNSCC. Our study identified a significant up-regulation of circPRMT5 in the salivary exosomes of patients with HNSCC. Conversely, a significant down-regulation of circPRMT5 was observed in the salivary exosomes of patients one month postoperative compared to preoperative levels, underscoring its critical diagnostic and monitoring utility. Furthermore, elevated circPRMT5 levels in salivary exosomes were associated with a higher likelihood of cervical lymph node metastasis and advanced T stage in patients. These findings indicate that circPRMT5 possesses substantial potential for diagnostic, monitoring, and predictive applications.

Nevertheless, our study is subject to certain limitations. Primarily, the clinical sample size we obtained was insufficiently large. While the results achieved statistical significance and support our conclusions, employing a larger multicenter clinical sample could potentially enhance the robustness and generalizability of our findings. Additionally, due to the complexity of head and neck cancer (HNC), our research concentrated on HNSCC, which has the highest incidence, rather than encompassing the diagnosis of all HNC types. Future investigations could explore the diagnostic value of circPRMT5 for HNC in its entirety, should the opportunity arise. Thirdly, the atrophy of salivary glands resulting from postoperative radiotherapy and other factors in numerous HNSCC patients poses significant challenges in saliva collection. Consequently, we were unable to obtain sufficient postoperative saliva samples to assess the long-term monitoring capability of circPRMT5 on patient cancer outcomes, which represents a limitation of this study.

Conclusion

In conclusion, our study demonstrated that circPRMT5 is upregulated in HNSCC tumor tissues and facilitates HNSCC progression *in vitro* and *in vivo*. Mechanistically, circPRMT5 directly interacts with and stabilizes the IGF2BP3 protein, thereby enhancing IGF2BP3-mediated SERPINE1 expression through increased stability of SERPINE1 mRNA. Furthermore, circPRMT5 was evaluated in the saliva exosomes of HNSCC patients, which showed a positive correlation

with lymph node metastasis and advanced T stage, indicating its potential diagnostic value. Future research should consider circPRMT5 as a promising target for diagnostic and therapeutic strategies in HNSCC.

Acknowledgments

This work was supported by grants from the National Natural Science Foundation of China (No.82102691) and the Guangzhou Science and Technology Planning Project (202201010895).

Disclosure

The authors report no conflicts of interest in this work.

References

1. Cramer JD, Burtneß B, Le QT, Ferris RL. The changing therapeutic landscape of head and neck cancer. *Nat Rev Clin Oncol*. 2019;16(11):669–683. doi:10.1038/s41571-019-0227-z
2. Johnson DE, Burtneß B, Leemans CR, Lui VVY, Bauman JE, Grandis JR. Head and neck squamous cell carcinoma. *Nat Rev Dis Primers*. 2020;6(1):92. doi:10.1038/s41572-020-00224-3
3. Bray F, Ferlay J, Soerjomataram I, Siegel RL, Torre LA, Jemal A. Global cancer statistics 2018: GLOBOCAN estimates of incidence and mortality worldwide for 36 cancers in 185 countries. *CA Cancer J Clin*. 2018;68(6):394–424. doi:10.3322/caac.21492
4. Zhou WY, Cai ZR, Liu J, Wang DS, Ju HQ, Xu RH. Circular RNA: metabolism, functions and interactions with proteins. *Mol Cancer*. 2020;19(1). doi:10.1186/s12943-020-01286-3
5. Huang AQ, Zheng HX, Wu ZY, Chen MS, Huang YL. Circular RNA-protein interactions: functions, mechanisms, and identification. *Theranostics*. 2020;10(8):3503–3517. doi:10.7150/thno.42174
6. Lei M, Zheng GT, Ning QQ, Zheng JN, Dong D. Translation and functional roles of circular RNAs in human cancer. *Mol Cancer*. 2020;19(1). doi:10.1186/s12943-020-1135-7
7. Thomson DW, Dinger ME. Endogenous microRNA sponges: evidence and controversy. *Nat Rev Genet*. 2016;17(5):272–283. doi:10.1038/nrg.2016.20
8. Wang Z, Sun AQ, Yan AH, et al. Circular RNA MTCL1 promotes advanced laryngeal squamous cell carcinoma progression by inhibiting C1QBP ubiquitin degradation and mediating beta-catenin activation. *Mol Cancer*. 2022;21(1). doi:10.1186/s12943-022-01570-4
9. Chen S, Li K, Guo JW, et al. circNEIL3 inhibits tumor metastasis through recruiting the E3 ubiquitin ligase Nedd4L to degrade YBX1. *Proc Natl Acad Sci U S A*. 2023;120(13).
10. Kalluri R, LeBleu VS. The biology, function, and biomedical applications of exosomes. *Science*. 2020;367(6478):640. doi:10.1126/science.aau6977
11. Kalluri R. The biology and function of exosomes in cancer. *J Clin Invest*. 2016;126(4):1208–1215. doi:10.1172/JCI81135
12. Han T, Chen LJ, Li KR, et al. Significant CircRNAs in liver cancer stem cell exosomes: mediator of malignant propagation in liver cancer? *Mol Cancer*. 2023;22(1). doi:10.1186/s12943-023-01891-y
13. Zhang YY, Luo JY, Yang WK, Ye WC. CircRNAs in colorectal cancer: potential biomarkers and therapeutic targets. *Cell Death Dis*. 2023;14(6).
14. Chen X, Chen RX, Wei WS, et al. PRMT5 circular RNA promotes metastasis of urothelial carcinoma of the bladder through sponging miR-30c to induce epithelial-mesenchymal transition. *Clin Cancer Res*. 2018;24(24):6319–6330. doi:10.1158/1078-0432.CCR-18-1270
15. Pang J, Ye LW, Zhao D, Zhao D, Chen QW. Circular RNA PRMT5 confers cisplatin-resistance via miR-4458/REV3L axis in non-small-cell lung cancer. *Cell Biol Int*. 2020;44(12):2416–2426. doi:10.1002/cbin.11449
16. Fan ZN, He LH, Li MX, et al. Targeting methyltransferase PRMT5 retards the carcinogenesis and metastasis of HNSCC via epigenetically inhibiting Twist1 transcription. *Neoplasia*. 2020;22(11):617–629. doi:10.1016/j.neo.2020.09.004
17. Chandrashekar DS, Karthikeyan SK, Korla PK, et al. UALCAN: an update to the integrated cancer data analysis platform. *Neoplasia*. 2022;25:18–27. doi:10.1016/j.neo.2022.01.001
18. Chandrashekar DS, Bashel B, Balasubramanya SAH, et al. UALCAN: a portal for facilitating tumor subgroup gene expression and survival analyses. *Neoplasia*. 2017;19(8):649–658. doi:10.1016/j.neo.2017.05.002
19. Li BT, Zhu LL, Lu CL, et al. circNDUFB2 inhibits non-small cell lung cancer progression via destabilizing IGF2BPs and activating anti-tumor immunity. *Nat Commun*. 2021;12(1). doi:10.1038/s41467-021-24109-5
20. Li K, Guo J, Ming Y, et al. A circular RNA activated by TGFβ promotes tumor metastasis through enhancing IGF2BP3-mediated PDPN mRNA stability. *Nat Commun*. 2023;14(1):6876. doi:10.1038/s41467-023-42571-1
21. Ding Z, Guo L, Deng Z, Li P. Circ-PRMT5 enhances the proliferation, migration and glycolysis of hepatoma cells by targeting miR-188-5p/HK2 axis. *Ann Hepatol*. 2020;19(3):269–279. doi:10.1016/j.aohp.2020.01.002
22. Liu Y, Jiang H, Hu K, et al. CircPRMT5 promotes progression of osteosarcoma by recruiting CNBP to regulate the translation and stability of CDK6 mRNA. *PLoS One*. 2024;19(4):e0298947. doi:10.1371/journal.pone.0298947
23. Kristensen LS, Andersen MS, Stagsted LVW, Ebbesen KK, Hansen TB, Kjems J. The biogenesis, biology and characterization of circular RNAs. *Nat Rev Genet*. 2019;20(11):675–691. doi:10.1038/s41576-019-0158-7
24. Pan Z, Zhao R, Li B, et al. EWSR1-induced circNEIL3 promotes glioma progression and exosome-mediated macrophage immunosuppressive polarization via stabilizing IGF2BP3. *Mol Cancer*. 2022;21(1):16. doi:10.1186/s12943-021-01485-6
25. Ma Q, Yang F, Huang B, et al. CircARID1A binds to IGF2BP3 in gastric cancer and promotes cancer proliferation by forming a circARID1A-IGF2BP3-SLC7A5 RNA-protein ternary complex. *J Exp Clin Cancer Res*. 2022;41(1):251. doi:10.1186/s13046-022-02466-3
26. Lv X, Huang H, Feng H, Wei Z. Circ-MMP2 (circ-0039411) induced by FOXM1 promotes the proliferation and migration of lung adenocarcinoma cells *in vitro* and *in vivo*. *Cell Death Dis*. 2020;11(6):426. doi:10.1038/s41419-020-2628-4
27. Du M, Peng Y, Li Y, et al. MYC-activated RNA N6-methyladenosine reader IGF2BP3 promotes cell proliferation and metastasis in nasopharyngeal carcinoma. *Cell Death Discov*. 2022;8(1):53. doi:10.1038/s41420-022-00844-6

28. Ying Y, Ma X, Fang J, et al. EGR2-mediated regulation of m(6)A reader IGF2BP proteins drive RCC tumorigenesis and metastasis via enhancing S1PR3 mRNA stabilization. *Cell Death Dis.* 2021;12(8):750. doi:10.1038/s41419-021-04038-3
29. Gu Y, Niu S, Wang Y, et al. DMDMR-mediated regulation of m(6)A-modified CDK4 by m(6)A reader IGF2BP3 drives ccRCC progression. *Cancer Res.* 2021;81(4):923–934. doi:10.1158/0008-5472.CAN-20-1619
30. Li S, Cha J, Kim J, et al. Insulin-like growth factor II mRNA-binding protein 3: a novel prognostic biomarker for oral squamous cell carcinoma. *Head Neck.* 2011;33(3):368–374. doi:10.1002/hed.21457
31. Lin CY, Chen ST, Jeng YM, et al. Insulin-like growth factor II mRNA-binding protein 3 expression promotes tumor formation and invasion and predicts poor prognosis in oral squamous cell carcinoma. *J Oral Pathol Med.* 2011;40(9):699–705. doi:10.1111/j.1600-0714.2011.01019.x
32. Yang L, Yan B, Qu L, et al. IGF2BP3 regulates TMA7-mediated autophagy and cisplatin resistance in laryngeal cancer via m6A RNA methylation. *Int J Biol Sci.* 2023;19(5):1382–1400. doi:10.7150/ijbs.80921
33. Liu J, Jiang X, Zou A, et al. circIGHG-induced epithelial-to-mesenchymal transition promotes oral squamous cell carcinoma progression via miR-142-5p/IGF2BP3 signaling. *Cancer Res.* 2021;81(2):344–355. doi:10.1158/0008-5472.CAN-20-0554
34. Czekay RP, Higgins CE, Aydin HB, et al. SERPINE1: role in cholangiocarcinoma progression and a therapeutic target in the desmoplastic microenvironment. *Cells.* 2024;13(10):796. doi:10.3390/cells13100796
35. Kim WT, Mun JY, Baek SW, et al. Secretory SERPINE1 expression is increased by antiplatelet therapy, inducing MMP1 expression and increasing colon cancer metastasis. *Int J Mol Sci.* 2022;23(17).
36. Zhang D, Zhang JW, Xu H, et al. Therapy-induced senescent tumor cell-derived extracellular vesicles promote colorectal cancer progression through SERPINE1-mediated NF- κ B p65 nuclear translocation. *Mol Cancer.* 2024;23(1):70. doi:10.1186/s12943-024-01985-1
37. Hu Q, Peng J, Chen X, et al. Obesity and genes related to lipid metabolism predict poor survival in oral squamous cell carcinoma. *Oral Oncol.* 2019;89:14–22. doi:10.1016/j.oraloncology.2018.12.006
38. Wei WF, Zhou HL, Chen PY, et al. Cancer-associated fibroblast-derived PAI-1 promotes lymphatic metastasis via the induction of EndoMT in lymphatic endothelial cells. *J Exp Clin Cancer Res.* 2023;42(1):160. doi:10.1186/s13046-023-02714-0
39. Kisoda S, Shao W, Fujiwara N, et al. Prognostic value of partial EMT-related genes in head and neck squamous cell carcinoma by a bioinformatic analysis. *Oral Dis.* 2020;26(6):1149–1156. doi:10.1111/odi.13351
40. Li X, Wang C, Zhang H, et al. circFND3B accelerates vasculature formation and metastasis in oral squamous cell carcinoma. *Cancer Res.* 2023;83(9):1459–1475. doi:10.1158/0008-5472.CAN-22-2585
41. Alix-Panabières C, Pantel K. Liquid biopsy: from discovery to clinical application. *Cancer Discov.* 2021;11(4):858–873. doi:10.1158/2159-8290.CD-20-1311
42. Yu D, Li Y, Wang M, et al. Exosomes as a new frontier of cancer liquid biopsy. *Mol Cancer.* 2022;21(1):56. doi:10.1186/s12943-022-01509-9
43. Street JM, Barran PE, Mackay CL, et al. Identification and proteomic profiling of exosomes in human cerebrospinal fluid. *J Transl Med.* 2012;10. doi:10.1186/1479-5876-10-5
44. Hoshino A, Costa-Silva B, Shen TL, et al. Tumour exosome integrins determine organotropic metastasis. *Nature.* 2015;527(7578):329. doi:10.1038/nature15756
45. Nimir M, Ma YF, Jeffreys SA, et al. Detection of AR-V7 in liquid biopsies of castrate resistant prostate cancer patients: a comparison of AR-V7 analysis in circulating tumor cells, circulating tumor RNA and exosomes. *Cells.* 2019;8(7):688. doi:10.3390/cells8070688
46. Li L, Li C, Wang SX, et al. Exosomes derived from hypoxic oral squamous cell carcinoma cells deliver miR-21 to normoxic cells to elicit a prometastatic phenotype. *Cancer Res.* 2016;76(7):1770–1780. doi:10.1158/0008-5472.CAN-15-1625
47. Lu J, Liu QH, Wang F, et al. Exosomal miR-9 inhibits angiogenesis by targeting MDK and regulating PDK/AKT pathway in nasopharyngeal carcinoma. *J Exp Clin Canc Res.* 2018;37. doi:10.1186/s13046-018-0814-3
48. Bao LL, You B, Shi S, et al. Metastasis-associated miR-23a from nasopharyngeal carcinoma-derived exosomes mediates angiogenesis by repressing a novel target gene TSGA10. *Oncogene.* 2018;37(21):2873–2889. doi:10.1038/s41388-018-0183-6
49. He L, Ping F, Fan ZN, et al. Salivary exosomal miR-24-3p serves as a potential detective biomarker for oral squamous cell carcinoma screening. *Biomed Pharmacother.* 2020;121:109553. doi:10.1016/j.biopha.2019.109553

International Journal of Nanomedicine

Publish your work in this journal

The International Journal of Nanomedicine is an international, peer-reviewed journal focusing on the application of nanotechnology in diagnostics, therapeutics, and drug delivery systems throughout the biomedical field. This journal is indexed on PubMed Central, MedLine, CAS, SciSearch®, Current Contents®/Clinical Medicine, Journal Citation Reports/Science Edition, EMBase, Scopus and the Elsevier Bibliographic databases. The manuscript management system is completely online and includes a very quick and fair peer-review system, which is all easy to use. Visit <http://www.dovepress.com/testimonials.php> to read real quotes from published authors.

Submit your manuscript here: <https://www.dovepress.com/international-journal-of-nanomedicine-journal>

Dovepress
Taylor & Francis Group